

AUTONOMOUS ORNITHOPTER USING LEAPING MECHANISM FOR LAUNCHING

R Hesin Raj¹, Sachin S², Adersh S³, Gautham Krishna S⁴, Dr. Bindu S.S⁵

¹⁻⁴Student, Dept. of Mechanical Engineering, Rajadhani Institute of Engineering and Technology, Kerala, India

⁵Head of Dept., Dept. of Mechanical Engineering, Rajadhani Institute of Engineering and Technology, Kerala, India

Abstract - This paper presents the design and simulation of the leaping maneuver for an ornithopter inspired by birds. Most flying bird's lift-off for flight from standing or perching position at low airspeed with the usage of their hind limbs. A lightweight 4-bar limb mechanism has been designed using three-position dimensional synthesis by motion generation in MSC.ADAMS, MATLAB/Simulink. Graphical methods and kinematic synthesis have been used to determine the prescribed lift-off maneuvers. The weight at the linkage sections is reduced by using carbon fibre prepreg material in order to have better strength and lesser weight. The leaping limb has been tested with an efficient aerodynamic model that accurately predicts unsteady flapping wing aerodynamic characteristics just after launching. Force analysis has been done in order to determine its transition from limbs to wings. While having a pitch angle of 45 degrees with an initial leaping velocity of 12 m/s, the 30-gram flapping-wing aerial vehicle gains more momentum when compared to another test with the same pitch angle but with an increased flapping frequency of 5 Hz and initial velocity of 11m/s is conducted which makes it to attain a steady-state flight which almost equals the value of its initial velocity.

Key Words: Ornithopter, Biomimetics, Lift-off, Linkage Synthesis, Aerodynamic Model, Leaping Mechanism

1. INTRODUCTION

Over the years, the primary flight characteristics of birds such as swift take-off, flight actions, hovering, and gliding has inspired plenty of research on robotic flyers based on biomimicry, termed as Flapping Wing Aerial Vehicles (FWAVs) or Ornithopters [1]. Adopting such flapping mechanisms on robotic flyers would suit them in stealth operations demanding agility, efficiency, and maneuverability, and can also be used for e-commerce businesses. To sufficiently meet their efficacy, ornithopters need to autonomously lift off, fly and make a landing on surfaces like their natural counterparts.

Most of the researches done till today majorly focuses on the various wing, tail, and flapping mechanism designs and configurations to achieve different flight modes. However, most of the ornithopter's lift-off is by human aid, either by throwing it into the air or by using a catapult for micro aerial vehicles. This launching technique restricts their autonomous capabilities especially when needed to land and re-launch from remote, inaccessible areas or even meet their expectations in swarm robotics applications. Most of the

birds lift off using their limbs which provide the initial impulse for flight [2,3]. Starting flight by leaping increases air circulation over the wings, provides additional lift at low airspeeds encountered just after lift-off, and gives enough ground clearance for the wings to flap [3].

Quite a few Literature Surveys are done on Flapping Wing UAVs. However, efforts to achieve terrestrial-aerial transitions have been shown in multi-modal robots of land and air mobility. For instance, MALV in [4] could make transitions from crawling to flight by a legged run, although being launched by human aid shows it was still not completely autonomous. BOLT in [5] could get to float in the air also by a legged run within a short distance assisted by wings. The combined working of wings and limbs reduced power efficiency in both modes. Further, work in [6] intricate a coordinated launch at a certain desired angle between two robotic platforms at minimum velocity. However, due to quite a few constraints in this setup, at times it incurred unsuccessful launches. Therefore, launching Ornithopter's by running on limbs proved intricate, heavy, and delicate. A memory alloy-actuated catapult system for lift-off has been designed and developed in [6], though it lacked continuous operation since it was removable from the ornithopter's body. Micro aerial vehicles like in [7] achieved stable vertical lift-off by high-frequency wing thrust, a technique that suits insect flyers but would be energy inefficient for large-sized aerial vehicles.

Traditionally leaping mechanism in robots was used against obstacles and rough terrain [8,9], but later when there was a need for leaping long distances, it led to the use of leap-gliding which uses un-actuated wings to increase leaping action and decrease landing impact [10]. This concept of leap-gliding provides useful insights into this project, but unlike leap-gliders, leaping for ornithopter's is emphasized to start flight for actuated wings, very similar to that of flying birds. Also based on the fact that birds maximize their initial flight velocity using limb thrust as compared to the downstroke of their wings as given in [11]. The leaping limb herein, inspired by the rock pigeon, is tested with an efficient aerodynamic model based on Modified Strip Theory in [12] with certain developments in [13] suit better to practical situations. Quite a few numbers of design iterations have been done to establish successful transition of forces from limbs to the wings.

2. HOW DOES A BIRD FLY?

An experiment conducted on *Columba Livia*, a rock pigeon, reveals that during liftoff, their limbs are separated from the ground even before the first downstroke of its wing which means that it is entirely reliant on limb thrust and no lift generation is concerned [11]. The movement is mainly influenced by the forward motion of centre of mass through head and neck movements. The analysis showed that the reaction force from the ground was about quadruple of its weight. Usually, birds lift off in three stages i.e., limb thrust, clap-and-fling, and steady-state flight [3]. Birds initially squat down to minimum retracted angle, then extend their limbs within a quick fraction thus developing a launch force that projects the bird in the desired direction as shown in the Fig-1.

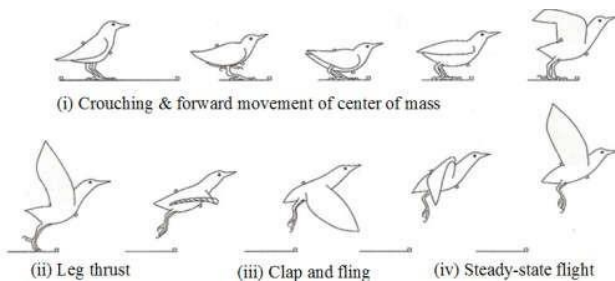


Fig-1: Step-by-step stages of leaping maneuver

3. BIOMIMETIC DESIGN

3.1 Fundamental Design

Design characteristics such as weight, power, and aerodynamic constraints led to arrest important aspects of birds that enable successful lift-off from theoretical bio-inspiration as in [14]. Generally, Rock pigeon's limb bones are hollow, light, and strong. The four basic parts of a bird's limb are the femur, tibia, tarsus, and toes as seen in Fig-2 (a). The four toes are controlled by a framework of muscles from the tibia, whereas the taurus contain no muscle. Our instance of bio-mimicry draws more importance from the bird's leaping maneuver than its biological features, and those are wide-angle variation, forward motion due to the centre of mass, and lift-off by limb thrust. The design in Fig-2 (b) perceives lift-off maneuver from a line projected through the body's centre of mass in a vertical plane, guided through some prescribed set of sequential positions. The design would mainly consist of tibia, taurus, and toes, and ignores Femur and a few minor segments on the toes. Muscles that are used for energy storage and movement are represented by torsion springs that deform, store elastic energy within, then release it as a whole for lift-off.

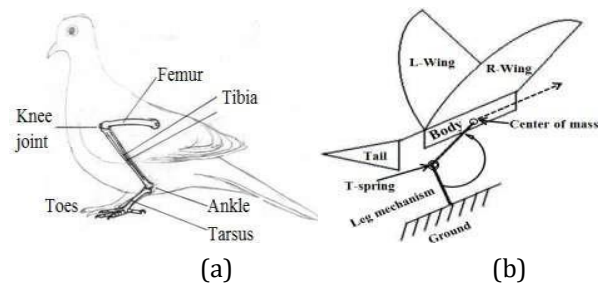


Fig-2: (a) Columba Livia's limb structure (b) Fundamental design of ornithopter lift-off maneuver

3.2 Intricate Design

It was necessary to observe some requirements in the preparatory stage to create a pragmatic and efficient design. The prior mentioned behaviors led to a design having simple, light, and strong support. The lift-off should be at an inclined angle with the resultant vector force resolved by the vertical and horizontal components. The net thrust force should pass through the centre of mass of the body. It should be able to perform an efficient transition from land to air in a quick, timely, and efficient manner and should also have wide-angle variation during leaping to release maximum kinetic energy.

Designs are rendered with the help of graphical method and analytical method.

3.2.1 Graphical Design

Fig-3 shows a three-position synthesis with a fixed pivot which has been used to accurately generate motion of the mechanism that would meet the above requirements in CATIA V5 software. The coordinates P_1 , P_2 , P_3 have been selected with lines projected from these points to direct the coupler from crouching position to lift-off position. Point Q_0 has been provisionally chosen at the origin as the centre point and regarded as foot joint. The centre point P_0 can be acquired with circle points P_1 , P_2 , P_3 . With the use of the inversion process, the location of circle point Q corresponding to centre Q_0 can be obtained. Fig-4 (a) shows the link drawn in horizontal position P_1 as regarded as the initial squatting position for the birds. Linkages of Grashof type III with dimensions in millimeters has been obtained as follows: ground-link $L_1=35$, crank $L_2= 30.10$, coupler $L_3= 53.11$, and rocker $L_4=48.01$.

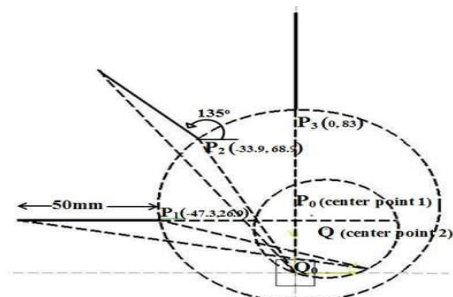


Fig-3: Detailed graphical drawing in CATIA V5

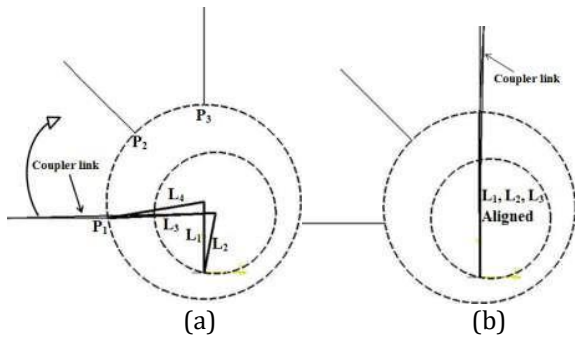


Fig-4: Link configurations (a) Horizontal and (b) Vertical

3.2.2 Analytical Design

The input and output angles are correlated using Freudenstein's equation in terms of link lengths a, b, c and d.

$$K1 \cos \theta - K2 \cos \psi + K3 = \cos(\theta - \psi) \quad (1)$$

Where, $K1 = da$; $K2 = dc$; and $K3 = 2ac(a^2 - b^2 + c^2 + d^2)$

The prior mentioned accuracy points are confirmed by synthesizing the linkage prescribed in linkage method. The joint coordinates A and B are obtained into horizontal and vertical components by drawing the linkage with the configuration shown in Fig-5 (a). Pythagoras theorem and trigonometric identities are applied and the equations are formulated as (1) [17]. $K1$, $K2$, and $K3$ can be evaluated using three equations as follows:

$$K1 \cos \theta_1 - K2 \cos \psi_1 + K3 = \cos(\theta_1 - \psi_1) \quad (2)$$

$$K1 \cos \theta_2 - K2 \cos \psi_2 + K3 = \cos(\theta_2 - \psi_2) \quad (3)$$

$$K1 \cos \theta_3 - K2 \cos \psi_3 + K3 = \cos(\theta_3 - \psi_3) \quad (4)$$

The values of $K1$, $K2$, and $K3$ are obtained as the functions of a/d , b/d , and c/d respectively using MATLAB by substituting angles for three arbitrary positions in (2), (3), and (4). Ground-link $L_1 = 35.0$, crank $L_2 = 30.08$, coupler $L_3 = 53.06$, and rocker $L_4 = 48.15$ were acquired in millimetres, and the measurements obtained graphically are verified. A 3D render with hollow circular cross-sections has been made with the help of CATIA V5 environment. The limb has been connected to the ornithopter.

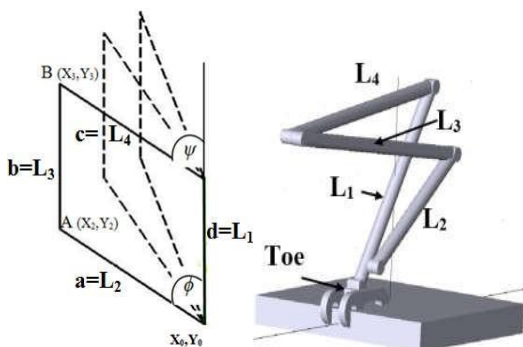


Fig-5: (a) Linkage Synthesis (b) 3D rendered model

4. AERODYNAMICS

The leaping limb is then attached and tested with an ornithopter that is designed aerodynamically based on Modified Strip Theory [12], in which each of its wings is divided into 12 equal strips, each of which is an aerofoil of finite width. The total lift and thrust forces of the flapping wings shown in Fig-6 are obtained by the span-wise integration of the sectional aerodynamic forces as shown in Fig-7. An advanced model of this in [13] is considered to have a high relative angle of attack and dynamic stalling effects that reflects realistic twisting and diving motion.

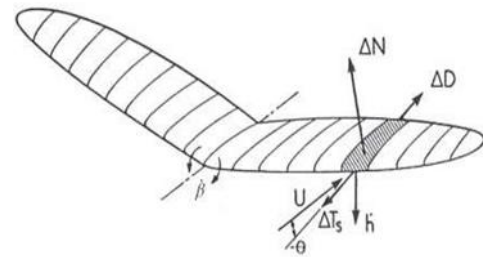


Fig-6: Aerodynamic forces acting on flapping wings

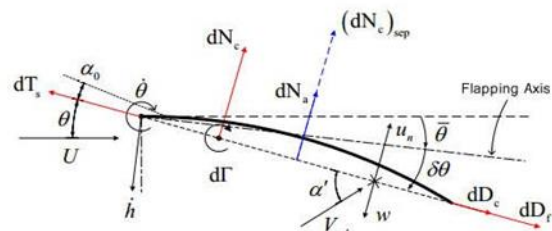


Fig-7: Motion variables and aerodynamic forces on wing section

Some important aerodynamic forces are directly described here, but in detail descriptions are in [12,13]. For attached flow conditions, the total normal force (dN) is:

$$dN = dN_a + dN_c \quad (5)$$

Where, dN_a and dN_c are normal apparent mass and circulatory forces respectively. Chord-wise forces comprises of camber force (dD_c), leading-edge suction force (dT_s) and friction drag due to viscosity (dD_f), thus total force (dF_a) is:

$$dF_a = dT_s - dD_c - dD_f \quad (6)$$

And now for separated flow, all of the chord wise forces are neglected and considering only normal forces as in [12]. The sections instantaneous lift and thrust forces are given as follows:

$$dL(t) = dN \cos \theta + dF_a \sin \theta \quad (7)$$

$$dT(t) = dF_a \cos \theta + dN \sin \theta \quad (8)$$

Where, θ represents the pitch angle of the chord with respect to the free stream velocity U . Thus, the span wise

integration gives the whole wing's instantaneous lift and thrust as follows:

$$L(t) = 2 \int_0^{b/2} \cos\beta dy \quad (9)$$

$$T(t) = 2 \int_0^{b/2} dT \quad (10)$$

Where β is the section's instantaneous dihedral angle.

5. WEIGHT DETERMINATION

The contemporary lift equation [2] was used to calculate the weight of the simulated model, where α , ρ , A , and V stand for lift coefficient, air density, wing area, and cruise velocity respectively.

$$L = \frac{1}{2} \alpha \rho V^2 A \quad (11)$$

During flight, the ornithopter's weight is supported by its wings. As a result, weight equals lift. For the goal of reducing induced drag, an elliptical wing form with an area of 12100 mm² was chosen. A flight speed of 10 m/s has been chosen as a rough estimate, with an air density of 1.25 kg/m³ around sea level. If the angle of attack θ is 1/22.5 radians in long-distance flight as same as in [2] and the lift coefficient, gives α a value of 0.873.

Analysis of the lift gives a weight of 0.660 Newton. The estimated weight of the motors, transmission system, onboard controls, body, and batteries are included in the overall weight. For a strong efficient leap the leg weight should be at least one-sixth of total body weight. Below, Table I outlines the model's parameters, whereas Fig-8 depicts the whole Dynamic model in MSC. ADAMS:

Table-1: Virtual model specification

Parameters	Value	Units
Wing area (A)	0.0121	m ²
Mean chord (c)	0.0752	m
Wing span (S)	0.4500	m
Body weight (w_b)	0.0550	kg
Leg weight (w_l)	0.0110	kg
Total weight (W)	0.660	N



Fig-8: MSC ADAMS 3D model

6. BIOMIMETIC DESIGN EVALUATION

6.1 Evaluation of Launching Mechanism

The proposed model for the launching mechanism has been customized using MSC.ADAMS software without the effect of lift from wings. The model weighs about 11 grams. The material chosen to make the mechanism is carbon fiber since it has a high strength to weight ratio and fatigue resistance. The lift-off velocity has been chosen as 10 m/s which yields spring rotational stiffness coefficient k of 1.6 Newton-meter per radian. The torsion spring's maximum angle of twist from equilibrium θ_{max} is 2.6 radians, and the preload torque is 4.32 Newton-meter. As a result, the elastic energy $E_l = \frac{1}{2} k(\theta_{max})$, which equivalent to 5.832 joules is enough to overcome wing aerodynamic drag, body inertia, and gravity. During leaping, thrust force directed from the leg's contact point with the ground travels through the ornithopter's centre of mass, resulting in a 45-degree leap angle that is generally constant. In this instance, an inclined lift-off is required to decrease energy losses owing to wing aerodynamic drag. As illustrated in the Fig-9, aligning legs along the longitudinal axis of flight after the lift-off lowers drag during flight.

As shown in Fig-10 (a), the model assumed a ballistic trajectory under gravity with a maximum height of 0.86 metres, which compensates for the absence of aerodynamic forces to generate lift for flight. Another test was carried out to see how lift from wings affected the leaping mechanism when it was turned off. Even at high frequencies, the model was found to be unable to produce adequate lift for lift-off. The launch velocity in Fig-10 (b) increases with an increment in kinetic energy indicated in Fig-10 (c) to a peak of 12.2 m/s in a brief time frame of 0.25 seconds. This sharp linear growth indicates a constant rate of acceleration. The greatest velocity corresponds to the time of leaping, which is five milliseconds. As the ornithopter declines, kinetic energy peaks at 0.81862 Newton-meter and then gradually decreases.

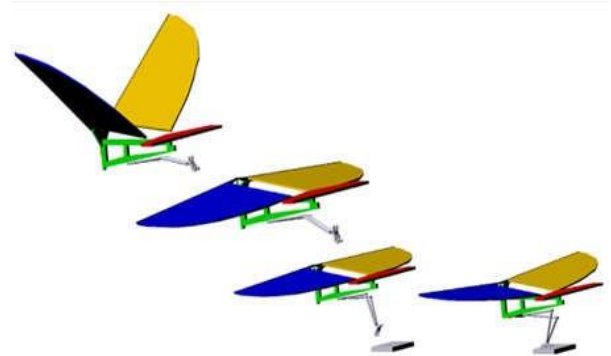


Fig-9: Leaping to steady state flight simulation

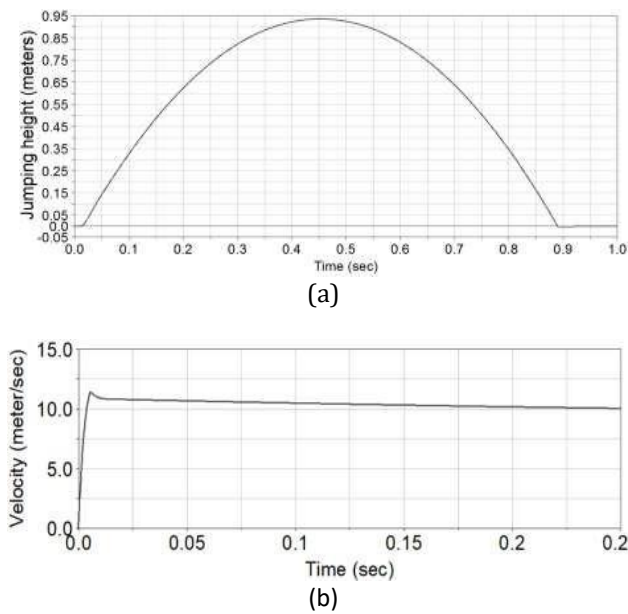


Fig-10: (a) Leaping height (b) Velocity vs Time (c) Kinetic energy vs Time

6.2 Evaluation of Flight with Leaping Mechanism

The ornithopter will shift towards steady-state aerodynamics after the lift-off. The simulation framework aims to determine the force transfer from limbs to wings while accounting for unstable aerodynamic effects. MSC.ADAMS generates outputs by modeling the structural dynamics of the ornithopter and the leaping limb. It connects to MATLAB/Simulink, which performs complicated numerical analysis of flight dynamics and supplies the necessary input forces. The flowchart in Fig-11 describes the process of modeling flight performance.

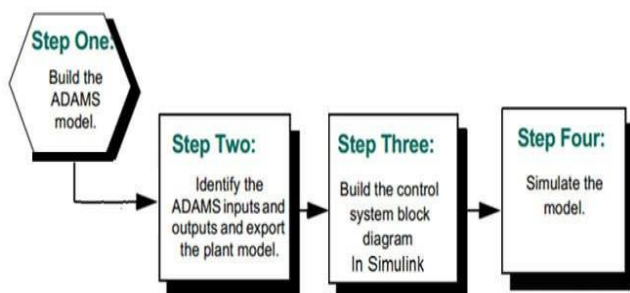


Fig-11: Simulation framework for ornithopter model

The computational study of unsteady aerodynamics of rigid elliptical wings as stated in table I was carried out using MATLAB, taking into account high relative angle of attack and dynamic stall effects at a frequency of 15 hertz, 10 m/s flight speed, and Aspect Ratio, AR of 4.8. The whole wingspan contains 192 input aerodynamic forces, with 8 forces operating on each strip. The goal was to use (9) and (10) to examine the lift and thrust coefficients produced by the wings at the specified parameters using (9) and (10).

Time-varying sinusoidal graphs are illustrated in Fig-12. In the connected flow range, the trough indicates up-stroke, while in the stall flow range, the crest represents down-stroke. The fact that the amplitudes are higher on the downstroke confirms that greater lift is created owing to aerodynamic loading in the downstroke than on the upstroke.

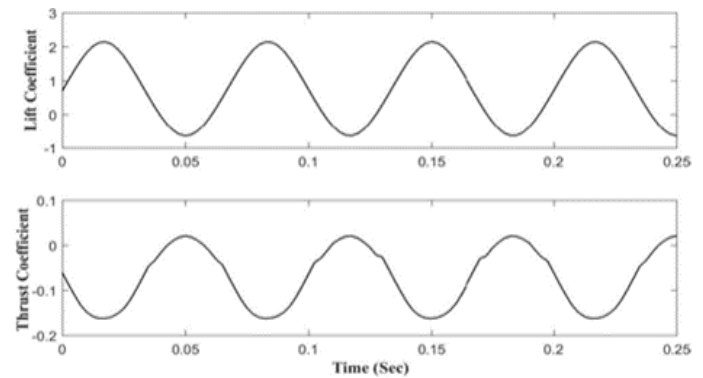
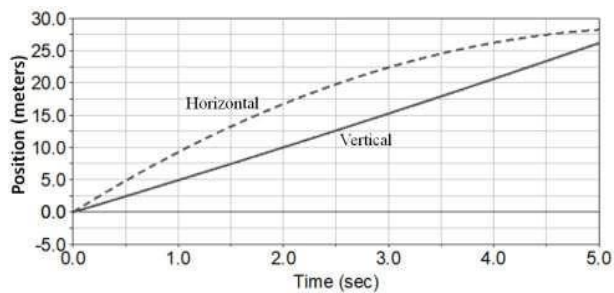


Fig-12: Coefficient of lift and thrust vs time

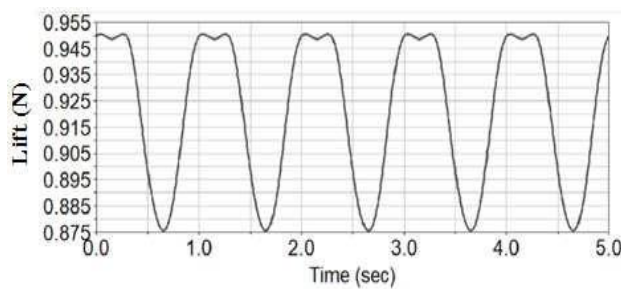
Forward velocity U , flapping frequency f , and a pitch angle of flapping axis relative to free stream velocity θ_a , were among the state variables in flight dynamics. Several design iterations were carried out, starting with a squatting stance and ending with a leap off for flight. In a Simulink S-Function mask, the flapping frequency, f was varied between 0.2 to 18 hertz, the flying speed, U from 0.05 to 20 m/s and the pitch angle, θ_a from 0 to 10 degrees. The goal was to establish a steady-state flight mode.

The vertical height grows exponentially with time at high flapping frequencies, resulting in speed variation. Therefore, the flapping frequency has been reduced to 1 hertz and the leaping velocity to 8.8 m/s in MSC.ADAMS. As illustrated in Fig-13 (a), a constant increase in height and distance occurs with a free stream velocity θ_a of 4.5 degrees and a flying speed U of 7.8 m/s. The model climbs at a pace of 4.8 m/s while gaining thrust at double that rate. The initial push generated by the limbs is correlated with the forward thrust velocity. After 5 seconds, it progressively declines. The lift plot illustrated in Fig.13 (b) displays a limited fluctuation in amplitude due to low θ_a . Continuous flapping wing movements create time-dependent pressures and moments, which might cause ripples on the crest.

Fig-14 (a) illustrates similar results with an initial leaping speed of 9.2 m/s and a flapping rate of 5 hertz following lift-off. Leaping momentum gives the ornithopter a steady flying speed of 8.2 m/s, with an ascension speed of 4.5 m/s. The corresponding lift plot from the wings is shown in Fig-14 (b). Considering the constant frequency and θ_a , it can be inferred that the initial lift-off velocity affects the steady-state flying speed.

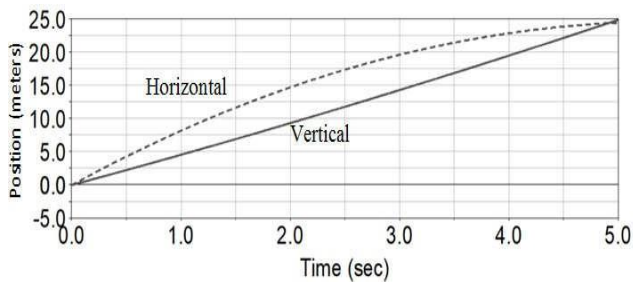


(a)

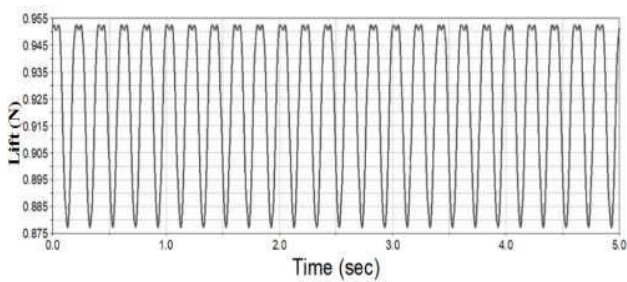


(b)

Fig. 13: (a) Vertical and horizontal displacements (b) Lift plot at 1Hz and 10m/s lift-off speed



(a)



(b)

Fig.14: (a) Vertical and horizontal displacements (b) Lift plot at 5 Hz and 9.2 m/s lift-off speed

In general, the MST-based model accurately predicted the performance of some flying configurations while failing to do so for others owing to unstable aerodynamics. Despite the model's challenges in reaching steady-state flight after lift-off at any given flight specification, modified strip theory with high angles of attack serves as a credible model for statistically forecasting flight performance of ornithopters.

7. CONCLUSION

The project proposes a leaping mechanism in ornithopters using limbs which is a potential prospect for launching robotic flyers. It was possible to use the notion of linkage synthesis via motion generation to accurately design and construct a system that matches lift-off behaviour in birds. It was decided to reduce the weight of the link cross-sections. An efficient model has been used to precisely estimate the aerodynamic performance of flapping wings after lift-off. The use of leaping limbs to launch robotic flyers improves their autonomy by removing the need for human intervention in the launching process. Their usefulness is determined by how well they adjust their movement to diverse settings on their own. The optimal synthesis of path-generating mechanisms, the use of flexible wings rather than stiff wings, and landing techniques, as well as their actual execution, may all be used in future works to attain better performance.

REFERENCES

- [1] Gerdes JW, Gupta SK, Wilkerson SA. "A review of bird-inspired flapping wing miniature air vehicle designs," *J Mech Robot* 2012.
- [2] Tennekes H. "The Simple Science of Flight: From Insects to Jumbo Jets," The MIT Press, Camb MA, 1997.
- [3] Heppner FH, Anderson JG. "Leg thrust important in flight take-off in the pigeon," *J Exp Biol* 1985;vol 114:pp 285-288.
- [4] Bachmann RJ, Boria FJ, Vaidyanathan R, Ifju PG, Quinn RD. "A biologically inspired micro-vehicle capable of aerial and terrestrial locomotion," *Mech Mach Theory* 2009;vol 44: pp 513-526.
- [5] Peterson K, Fearing RS. "Experimental dynamics of wing assisted running for a bipedal ornithopter," *Intell. Robots Syst. IROS 2011 IEEE/RSJ Int. Conf. On, IEEE;* 2011, p. 5080-5086.
- [6] Jianglong G, Shuping C, Long L, Zhongqiu Y, Yang W, Mingxu M. "An Autonomously Hopping-off Micro Raised-flapping-wing Air Vehicle," *Control Conf. CCC 2012 31st Chin., IEEE;* 2012, p. 4322-4327.
- [7] Keennon M, Klingebiel K, Won H, Andriukov A. Development of the nano hummingbird: "A tailless flapping wing micro air vehicle," *AIAA Aerosp. Sci. Meet., AIAA Reston, VA;* 2012, p. 1- 24.
- [8] Zaitsev V, Gvirsman O, Hanan UB, Weiss A, Ayali A, Kosa G. "A locust-inspired miniature jumping robot," *Bioinspir Biomim*, 2015.
- [9] Plecnik MM, Haldane DW, Yim JK, Fearing RS. "Design exploration and kinematic tuning of a power modulating jumping monopod," *J Mech Robot* 2017;9:011009.
- [10] Vidyasagar A, Zufferey J-C, Floreano D, Kovač M. "Performance analysis of jump-gliding locomotion for miniature robotics," *Bioinspir Biomim*, 2015.
- [11] Barata JM, Silva TJ, Neves FM, Silva AR. "Experimental Analysis of Forces During Take-Off of Birds," *AIAA Inf. Syst.-AIAA Infotech Aerosp.,* 2017, p. 1373.
- [12] DeLaurier JD. "An aerodynamic model for flapping-wing flight," *Aeronaut J* 1993, vol 97, pp 125-130.
- [13] Kim D-K, Lee J-S, Lee J-Y, Han J-H. "An aeroelastic analysis of a flexible flapping wing using modified strip

theory," Proc. SPIE 15th Annu. Symp. Smart Struct. Mater., vol. 6928, 2008, p. 692810.

- [14] Dietl J M, Garcia E. "Stability in ornithopter longitudinal flight dynamics". Journal of Guidance, Control, and Dynamics, 2008.
- [15] Andreas T. Pfeiffer¹, Jun-Seong Lee, Jae-Hung Han and Horst Baier. "Ornithopter flight simulation based on flexible multi-body dynamics", Technical University Munich, 2010.
- [16] M.Gang "An Autonomously Hopping-off Micro Raised-flapping-wing AirVehicle," Control Conf. CCC 2012 31st Chin., IEEE; 2012, p. 4322–4327.
- [17] Ghosal A. "The Freudenstein Equation and Design of Four-link Mechanisms," India, Indian Institute of Science, 2010.
- [18] Quinn RD, Nelson GM, Bachmann RJ, Kingsley DA, Offi JT, Allen TJ, et al. "Parallel complementary strategies for implementing biological principles into mobile robots," Int J Robot Res 2003, vol 22, pp169–186.